Angewandte Chemie
Eine Zeitschrift der Gesellschaft Deutscher Chemiker

Supporting Information

A Simple and Efficient Device and Method for Measuring the Kinetics of Gas-Producing Reactions

*Thierry K. Slot, N. Raveendran Shiju, and Gadi Rothenberg**

anie_201911005_sm_miscellaneous_information.pdf

Experimental details

Materials and instrumentation

Ammonia borane (>97%, Sigma Aldrich, 682098, 1g) and *n*-hexadecane (Fluka AG, Buchs SG, 138722, 1L) and 5% Ru/C (Alfa Aesar GmbH, 11748, 5g) were obtained from commercial sources. The bubble counter device housing and internal parts were printed on a Creality CR-10 3D printer using (poly)lactic acid (PLA, purchased from 123-3D.nl). Design files are available from the authors upon request.

Catalyst preparation

5% Ru/SiO_2 was prepared by wet impregnation: SiO_2 (100 mg, Grace Davison) was combined with a solution of $RuCl_3.H_2O$ in water and evaporated to dryness on an oilbath (85 °C) under continuous stirring. The resulting sample was dried in an oven at 120 °C for 2h after which the sample was reduced with 10% H_2/N_2 at 400 °C for 1h (ramprate 5 °C min^{-1}).

Sample preparation for bubble counter experiments

The catalyst, 5% Ru/C (2.5 mg), was suspended in water (7mL) inside a glass reactor (10mL) and ultrasonicated for 5 s. The reactor was attached to the reactor head which allows gasses and liquids to enter and leave the reactor through several syringe ports. (see description below). A stirring bean (3x8mm) was added to the reactor and the system was closed and prepared for reaction. A syringe was prepared with 400µL of 2M ammonia borane solution in water. The heating mantle was adjusted so it does not go above the liquid level inside the reactor. The temperature sensor was inserted and the purge gas line as well as the gas outlet was attached. The remaining ports were closed off. The reactor was stirred (400 rpm) and allowed to purge with nitrogen for 5 minutes.

Procedure for isothermal hydrolysis of ammonia borane.

Ammonia borane (2M aq soln, 0.40 mL) was loaded into a syringe equipped with a glass capillary that reaches into the reactor. The catalyst (2 mg) was suspended into water (6.0 mL) and a 8 mm stirring bean was added. The capillary was directly inserted into the liquid through one of the syringe ports. All remaining ports were closed. The reactor was then purged using a flowrate of 5 mL min^{-1} for 5 min. During purging, the reactor was heated to the reaction temperature after which the purging was stopped. After 5 seconds, the reactant was injected, resulting in some bubbles forming due to volume displacement. The gas production was then monitored until no more gas was produced.

Procedure for non-isothermal hydrolysis of ammonia borane

Ammonia borane (2M aq soln, 0.40 mL) was loaded into a syringe equipped with a glass capillary that reaches into the reactor. The catalyst (2 mg) was suspended into water (6.0 mL) and a 8 mm stirring bean was added. The capillary was directly inserted into the liquid through one of the syringe ports. All remaining ports were closed. The reactor was then purged using a flowrate of 5 mL min^{-1} for 5 min. During purging, the reactor was heated to the reaction temperature after which the purging was stopped. After 5 seconds, the reactant was injected, resulting in the formation of some bubbles due to volume displacement. The gas production was then monitored until no more gas was produced. Five seconds later, a ramp of 2°C/min was initiated. The sample was heated to 85 °C and held there for 5

min. Then the purge gas was turned on and heating was stopped. The sample was allowed to cool down to room temperature while being purged with gas.

Technical description

The machine consists of three parts: a metal bottom plate and two 3D printed parts that fit ontop of each other. The cover houses the detection unit (laser and LDR) and the display. The rest is installed on the bottom plate. The components on the bottom plate are: Arduino Uno, Arduino Mega, one stirring motor with magnets, a gas switch valve 12V, a 12V power supply, and the necessary connectors for both power and small signal in/output. Gas regulation is achieved by connecting the gas input through a regulating valve which is then led to the gas switch. From the switch, the gas line is connected to the reactor. We took care to avoid a large void volume in the gas lines as this adds to the void volume of the reactor. The bottom plate is depicted below. (Figure S**Figure S1**)

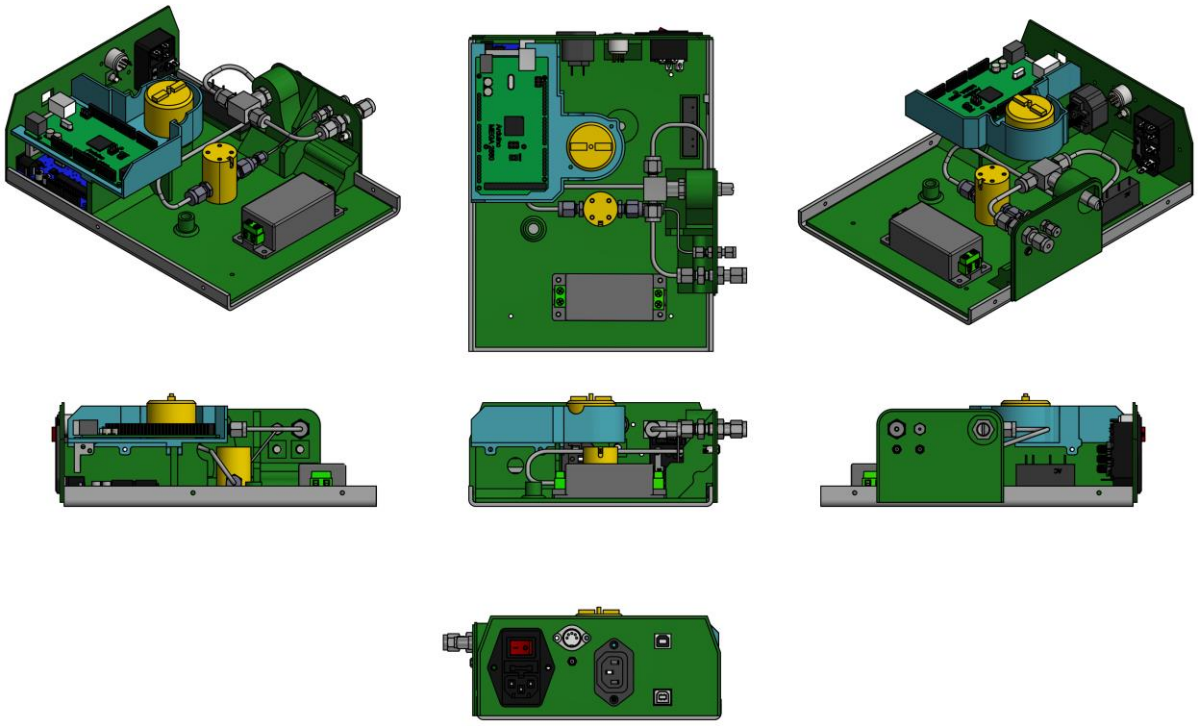

Figure S1: CAD views from the backplate assembly.

The top plate is detachable and is mounted on top of the backplate. It is fastened with four screws which are tapped into the aluminium backplate. It contains the detection assembly which can be positioned with a M8 thread. The display is a regular 2004A display equipped with a Hitachi HD44780U display driver.

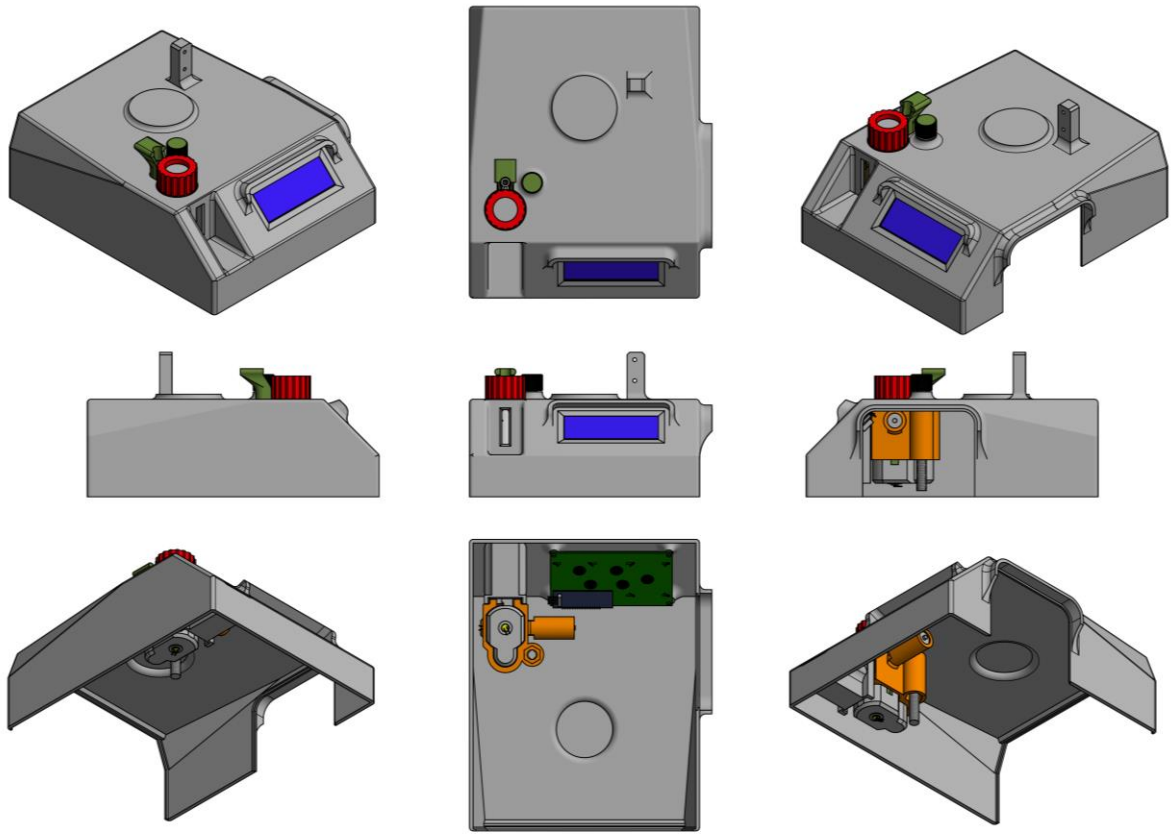

Figure S2: CAD views from the cover assembly.

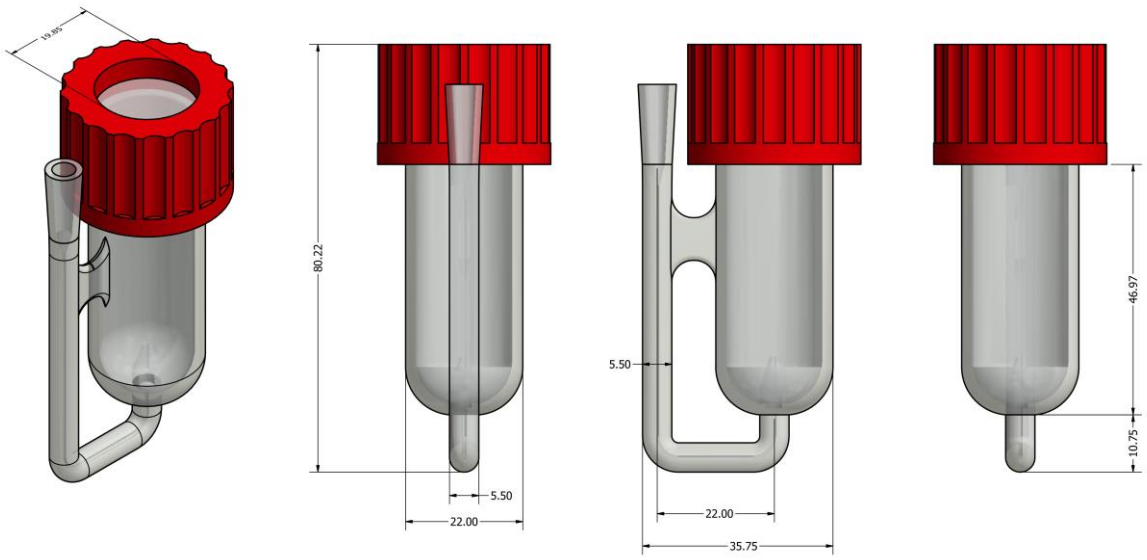

Figure S3: CAD views from the detection cell.

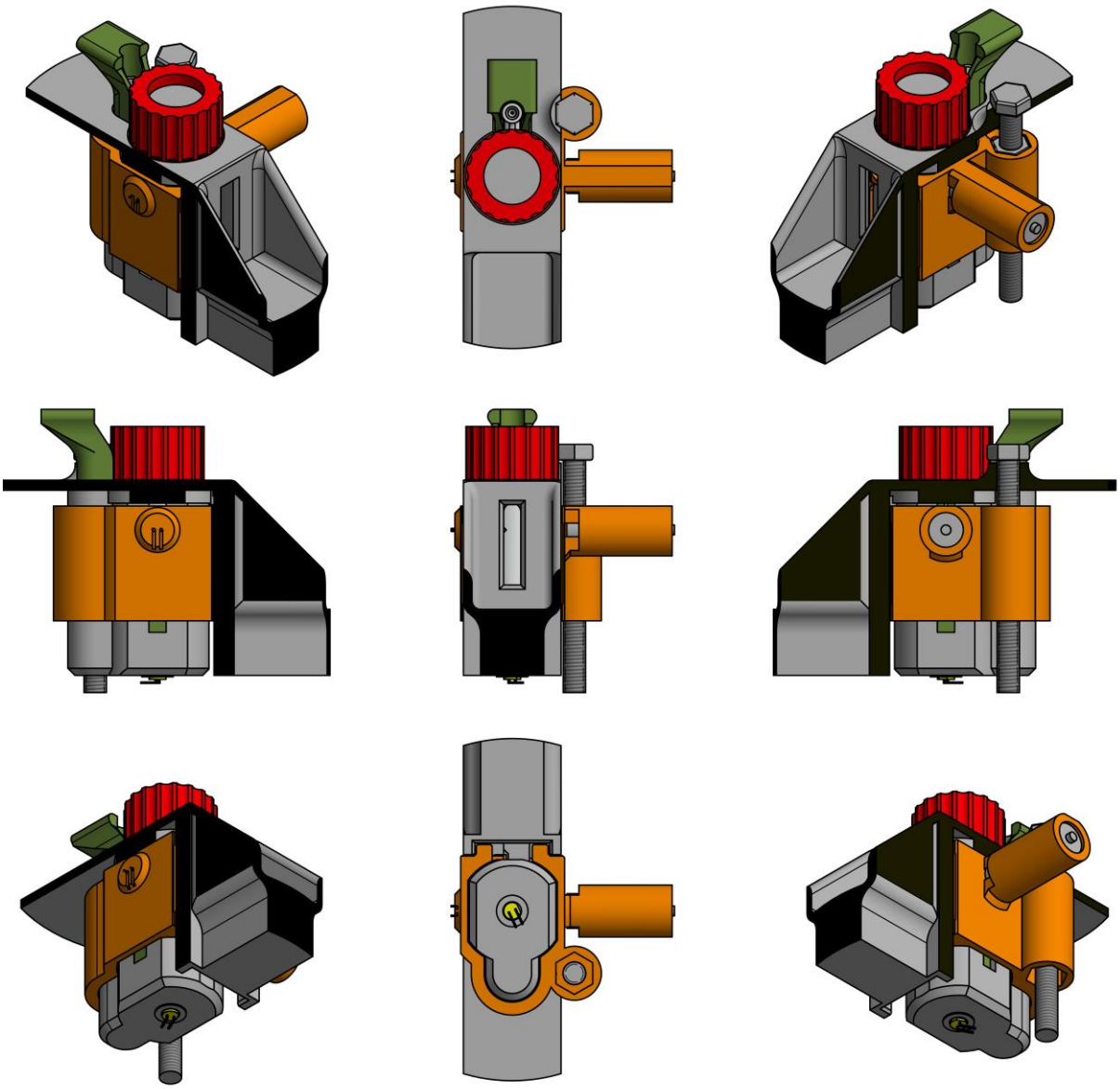

Figure S4: CAD views from the detection cell assembly in a cut-out section of the cover. The black regions represent cuts made for proper viewing of the assembly.

Bubble detection

The detection of bubbles is done by a 671 nm red laser module with a parallel beam width of 1.5 mm. Before it reaches the detection cell, the beam goes through a 1mm slit to let only the brightest part of the beam through. This makes the effective laser spot size is roughly 1 mm. The light sensor was positioned a few mm short of the focal point of the beam to allow a small spot size of 0.8 mm to fall on the LDR.

On average, the smallest bubbles forming in hexadecane have a diameter of around 2mm across the smallest axis of their ellipsoidal shape. This means the incident beam is large enough to detect these bubbles. Even if only part of the beam is reflected by the bubble, we still detect these bubbles because the detection algorithm identifies a bubble when >5% of the incident beam is reflected. In theory this means that the lower detection limit for bubbles is around 0.1 µL. In practice, these bubbles never

form because of the Laplace pressure that is required to form them. They rather expand into a larger bubble which is then most certainly detected when it leaves the nozzle.

The solubility of the gas in the detection cell and the reactor (as directed by Henry's law) can be of influence on the detection of bubbles, especially when the gas solubility is high and bubble formation progresses slowly. The gas can dissolve in the detection liquid therefore decrease the size of the bubble. However, all these effects can be mitigated by purging both sample and detection cell beforehand with the gas of analysis. This allows the gas concentrations to stabilize so there is no net effect on bubble size. For the same reason stirring is not needed in the detection cell. In the case of hydrogen, we do not see any significant differences with reactions when the system was pre-purged or not because of the low solubility and the relatively quick equilibration of H_2 in hexadecane. However, analysis of CO_2 from an aqueous reaction required extensive purging (up to 20 min) beforehand due to the high solubility of CO_2 in water.

Calibration experiments

Initially we tried to calculate bubble size from the beam interruption time (BIT). This indeed provided a reasonable correlation between BIT and bubble volume. Unfortunately, the BIT was highly dependent on surface tension (Figure S9), viscosity (Figure S10), laser height (Figure S11) and beam alignment, allowing for large variances in the BIT time. One other very valuable parameter is that we know how long it takes for a bubble to form, which translates into flowrate.

We observed that the flowrate has a large influence on the average bubble volume. Therefore, we chose to calibrate the detection cell by extruding 5 mL of air at different flowrates. A syringe pump was used in combination with a calibrated glass syringe. There appears to be a somewhat linear correlation between bubble volume and flowrate (Figure S5, left), however when we plot flowrate with different units (bubbles per second), we observe a linear relationship that seems to change at flowrates in excess of 12 mL s^{-1} (Figure S5, right). We hypothesize that above these flowrates the hydrodynamic drag of the bubble going upwards becomes more determining allowing for a larger increase in bubble volume. Another argument might be that the convectional flow inside the detection cell is somehow changed. Based on this data, we define the upper detection limit for hexadecane at 12 mL/min for hexadecane.

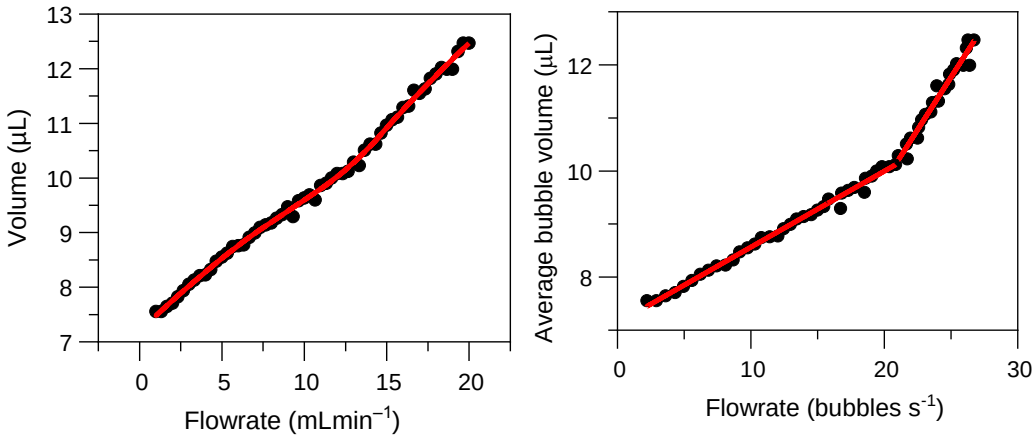

Figure S5: (a) average bubble volume versus flowrate (mL min^{-1}) in hexadecane. (b) average bubble volume versus flowrate in bubbles per second.

One additional reason for choosing the units in bubbles per second is that this can be easily calculated from the time between bubbles. The inverse of this time is the flowrate in bubbles s^{-1}. For practical purposes, we opted for a simple linear flow correction to only include the linear section up to 12 mL min^{-1}. However, if a large range of flowrate is necessary, the whole calibration curve can be used. For all our purposes a limit of 12 mL/min is more than enough to cover our experiments.

To verify our flow correction, we carried out additional measurements with known volumes (5mL) at different flowrates and calculated the final volume using the flow correction. (Figure S6)

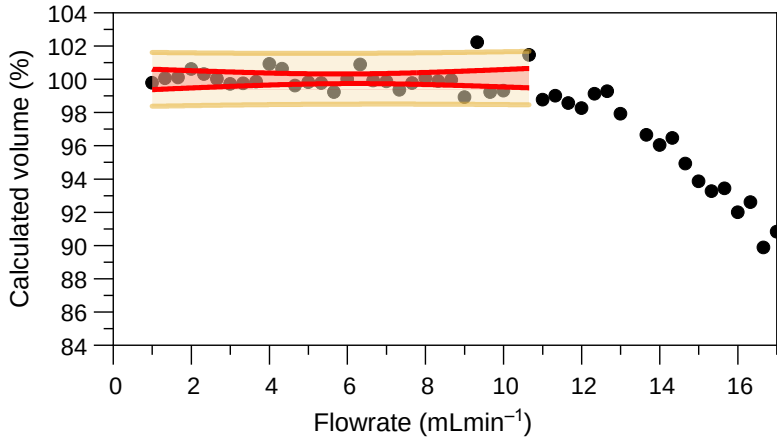

Figure S6: Flow-corrected volume (as percentage of the original volume) versus flowrate. 95% confidence and prediction intervals are represented in red and orange.

This shows that with flowrates up to 12 mL min^{-1} we get a final volume within 2% of the specified volume. This precision is comparable to mass spectrometry or GC. The instrumental precision of the syringe pump is unknown, so the actual instrument precision might be better.

One disadvantage of our system is that the summing of bubbles introduces errors that become larger when larger volumes (more bubbles) are being measured (error $\sim\sqrt{n}$). To mitigate this effect, a volume meter (or burette) can be connected to the gas outlet to correct the finally obtained volume. This makes the setup accurate, inexpensive and very versatile.

To investigate the influence of different gas types, we performed experiments with three different gasses: hydrogen, air and argon. The average bubble volume was not influenced significantly between the gasses or binary mixtures of them.

Blank experiments

Non isothermal experiments also bring about some difficulties. When using a ramp rate on reactions in liquid, one must also consider the increase in vapor pressure of the liquid. The resulting curve is a linear combination of a line (ideal gas law) and an exponential formula for vapor pressure. (eq. 3) The blank for water is shown in figure SX. For every sample that is being measured, a blank subtraction is done based on the temperature of the sample.

$$V = V_{gas\ expansion} + V_{vapor\ pressure} = (c_1 + c_2 x) + c_3 e^{-\frac{x}{c_4}} \qquad \text{(eq. 2)}$$

The gas production of a typical ammonia borane hydrolysis experiment is shown in figure 6a. Ammonia borane conversion is directly related to H_2 production. Hence, we can use the derivative of the volume-time curve as a measure of the reaction rate. Because we obtain so many data points, it is much easier to focus on the start of the reaction. Around this temperature, the substrate concentration remains practically constant, allowing us to treat the observed rates in this area as initial rates. Even as the reaction progresses, we can calculate the intrinsic reaction rate constant by using the known reaction order of the reaction. (eq. 3) Here *r* is the observed reaction rate, k_i is the intrinsic reaction rate, *[S]* is the substrate concentration and *n* is the rate order. Intrinsic rate is the rate the catalyst turns over substrate at unit molar concentrations of all reactants.

$$r = k_i[S]^n \qquad \text{(eq. 3)}$$

To construct an Arrhenius plot, we ideally need the intrinsic rate of the catalyst at different temperatures. This data is normally acquired by measuring the initial rate in a series of isothermal experiments at different temperatures. In our experimental setup this is not possible. As the substrate is consumed, the concentration S will drop, and the observed reaction rate will be lower than it was at the start of the reaction. However, if we know the reaction order we can correct for this. The intrinsic rate is calculated from the observed rate using eq. 3. For ammonia borane hydrolysis the reaction order was 0.35. Having this value close to zero helps us even more. This means that the dependence of the intrinsic rate on substrate concentration is small and therefore the intrinsic rate follows the observed rate more closely, even as the substrate is consumed, minimizing any error in this correction.

Purge function

One technical feature that proved necessary for non-isothermal experiments was the addition of a purge function. As the experiment finishes, the reactor cools down the gas in the reactor contracts. Without relief of this pressure, this will unenviably result in a transfer of the liquid from the detection cell to the reactor. The purge feature prevents this from happening. Another advantage is that at the reactor (and connected measuring cell) can be purged with a gas (ideally the gas that is being detected) to equalize the pressure in the reactor. This eliminates the initial pressurization necessary for pushing the gas inside the measuring cell. For the upside-down burette, this translates into a lead time in gas production that is dependent on the reaction rate of the catalyst.[22]

Figure S7: Relation between average bubble volume versus surface tension of a range of ethanol mixtures (0-40%, v/v).

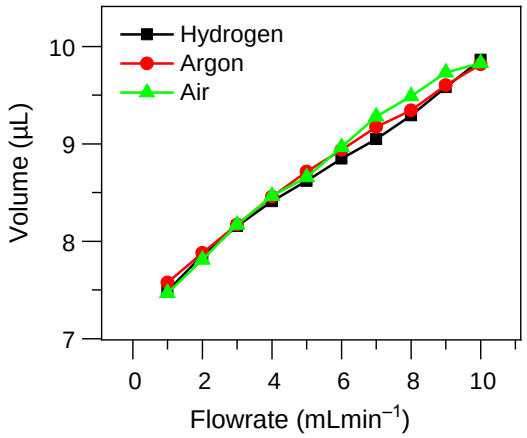

Figure S8: Average bubble volume at different flow rates using different density gases.

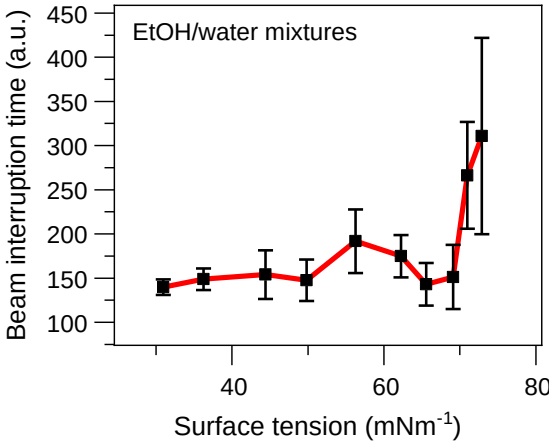

Figure S9: Surface tension (σ) plotted against the beam-interruption time (BIT). The error bars are multiplied 100 times for visibility.

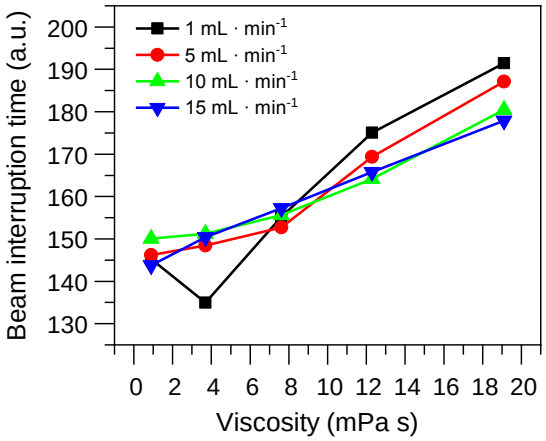

Figure S10: Influence of viscosity (μ) on the beam interruption time (BIT).

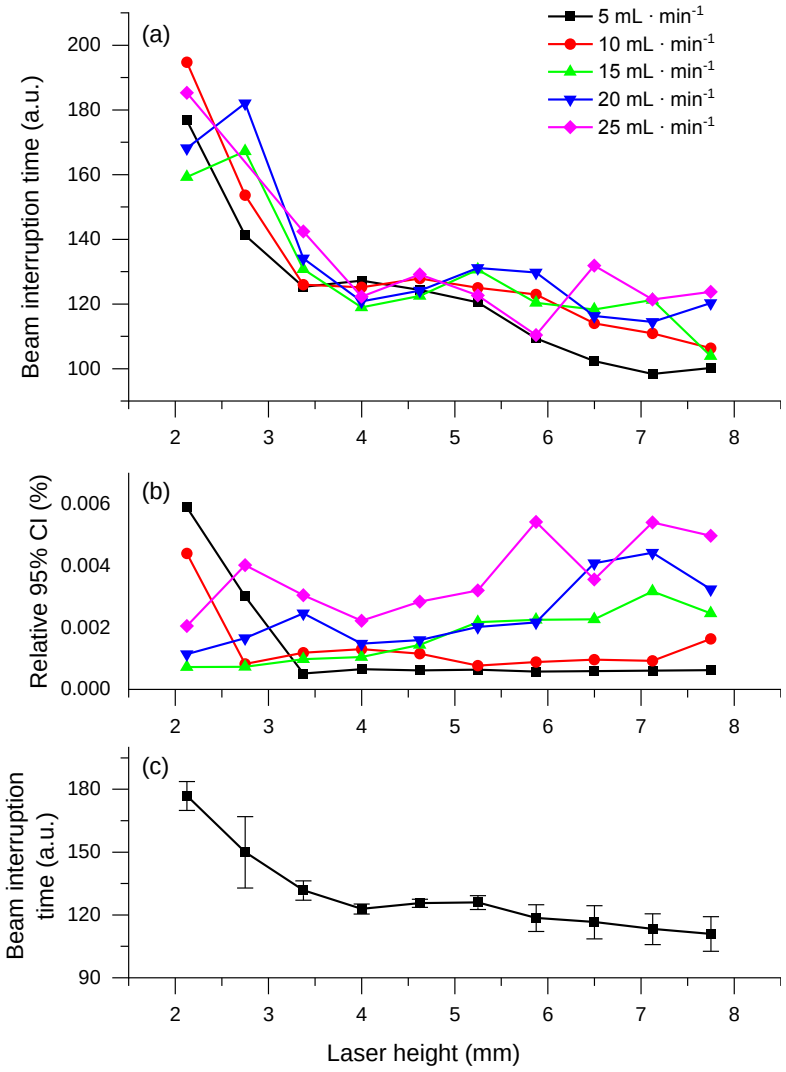

Figure S11. (a) Averaged beam interruption times (BIT) at various laser heights. (b) Relative 95% confidence intervals of the respective bubble sizes. (c) Averages and relative 95% confidence intervals (multiplied by 100 for visibility) of the bubble sizes over all flow rates.